Preprints of the 21st IFAC World Congress (Virtual)
Berlin, Germany, July 12-17, 2020

Parameter-dependent H_∞ control for MEMS gyroscopes: synthesis and analysis

Fabrício Saggin * **Jorge Ayala-Cuevas** * **Anton Korniienko** * **Gérard Scorletti** *

* *Ampère laboratory UMR CNRS 5005, Ecole Centrale de Lyon, Ecully, France (e-mail: fabricio.saggin@ec-lyon.fr).*

Abstract: The accuracy of micro-electro-mechanical systems (MEMS) gyroscopes is sensitive to variations of the drive mode resonance frequency ω_0. To tackle this problem, we propose an H_∞ control, which explicitly depends on ω_0 and guarantees, with reduced conservatism, a specified level of performance of the drive mode. We consider the design of continuous- and discrete-time controllers. We then propose a method based on the μ-analysis to validate the performance of drive mode control even if the frequency ω_0 is not perfectly measured. Numerical examples confirm the effectiveness of our approach.

Keywords: H-infinity control, Parametric variation, Performance analysis, Discretization.

1. INTRODUCTION

Micro-electro-mechanical systems (MEMS) gyroscopes are microscopic structures composed of a proof mass attached to a substrate by springs, creating two orthogonal resonant modes: the drive and sense ones. The oscillating signal $y(t)$ is created on the drive mode, such that, in the presence of an angular rate Ω (perpendicular to the resonant modes), a Coriolis force appears and produces oscillations on the sense mode $y_s(t)$. This force is proportional to the product $\Omega \cdot \dot{y}(t)$ and can be estimated by measuring the oscillations of the sense mode. Thus, if $y(t)$ is equal to a given reference $y_r(t)$, Ω is computed from $y_s(t)$ and $y_r(t)$. It is important to highlight that the gyroscope accuracy depends on how close the actual $y(t)$ is to $y_r(t)$. For further details, see *e.g.*, Saukoski (2008) and references therein. Therefore, in this paper, we restrict our attention to the drive mode oscillations control, which aims to keep $y(t)$ as close as possible to $y_r(t)$.

In general, the drive mode has high quality-factor, allowing to obtain a high signal-to-noise ratio when the drive mode operates close to its resonance frequency ω_0 (Sun et al., 2002). However, small drifts of ω_0 cause a significant loss of gain. So, in addition to a precise amplitude control, to reach high performance, the drive mode has to be operated with a frequency as close as possible to ω_0 (Egretzberger et al., 2010). The drifts of ω_0 are mainly due to changes in the sensor temperature (Xia et al., 2009), which are slow to ω_0.

In the literature, several control strategies are proposed to fulfill the above requirements. We mention the widespread architectures: automatic gain control (AGC) combined with phase-locked loop (PLL) (Sun et al., 2002; Egretzberger et al., 2010); and self-oscillating AGC (M'Closkey et al., 2001; Oboe et al., 2005). These solutions allow producing oscillations with controlled amplitude at the resonance frequency. However, the drawback of these nonlinear strategies is the lack of formal performance guarantees.

An alternative approach is to consider a classical feedback architecture, where a linear controller makes the output of the drive mode track a sinusoidal reference signal with frequency ω_0 and the desired amplitude. In this context, for a constant ω_0, celebrated design methods , as H_2 or H_∞, can be considered, giving performance guarantees (Skogestad and Postlethwaite, 2001). Nonetheless, when ω_0 changes, the reference signal and the controller have to be adapted for the new ω_0. To this end, similarly to the plant, the controller must be parameterized by ω_0. To the best of our knowledge, this approach is not considered for MEMS gyroscopes. Note that ω_0 can be measured, *e.g.*, through closed-loop identification techniques (Ljung, 1999).

The design of a parameter-dependent controller for a parameter-dependent plant is addressed by the so-called Linear Parameter-Varying (LPV) approaches. In our case, these approaches lead to conservative solutions or to a parameterization which can be too complex to be implemented in real-time. The conservatism comes from the fact that the parameter of interest is assumed to vary arbitrarily (Packard, 1994; Scorletti and El Ghaoui, 1998), whereas ω_0 varies slowly. On the other hand, Dinh et al. (2005) propose a nonconservative design method for constant parameter-dependent controller. However, the proposed controller parameterization is too complicated to be implemented in a limited-cost embedded processor.

In this work, we present, for the particular problem of MEMS gyroscopes (and similar ones), a parameter-dependent H_∞ controller design method. Our approach provides performance guarantees, reduced conservatism, and simple parameterization in the case where ω_0 is measured and constant. We propose two design methods: (i) for a continuous-time (CT) controller; and (ii) for a discrete-time (DT) controller. The former one is suitable for analog implementations or for digital implementations

* This work is supported by BPI France, through the NEXT4MEMS project, which aims to develop a new generation of MEMS sensors.

where the sampling period T_s is so small that the discretization effects (sampling and holding) may be neglected. Furthermore, this approach also gives the insight on the controller parameterization. The second method is suitable for digital implementations where the discretization effects have to be taken into consideration, which is often the case for MEMS gyroscopes.

The design of a CT parameter-dependent controller is based on the frequency/time normalization of the system, yielding to a straightforward parameterization for constant ω_0. The same strategy can be applied for the design of a DT parameter-dependent controller. However, approximations of the model have to be made. Then, it is crucial to investigate *a posteriori* the stability and the performance achieved by the DT parameter-dependent controller on the actual system for all possible values of ω_0. We propose to address this problem by using the robustness analysis framework (μ-analysis), where the approximation error and the frequency ω_0 are expressed as uncertainties. This problem is not standard since the uncertain model dependency on the uncertainties is nonrational. We then reveal how to recast this problem as a standard problem by using Taylor approximations. Furthermore, the proposed μ-analysis is based on the computation of the so-called μ upper-bound. The strong benefit is that stability and performance are also ensured for slow-time variations of ω_0 (Chou and Tits, 1995).

This paper is organized as follows. In Section 2, we state the problem under investigation. In Section 3, we present a solution in CT. In Section 4, we propose a method for designing a DT controller. In Section 5, we present a method for validating the closed-loop performance. In Section 6, numerical examples illustrate our approach. Conclusions and perspectives are drawn in Section 7.

Notation: $T_{a\to b}$ denotes the transfer from signal a to signal b. The $\star$ denotes the Redheffer (star) product (Skogestad and Postlethwaite, 2001). For a given linear time-invariant (LTI) system F, $\|F\|_\infty$ denotes its H_∞-norm. I_n is the identity matrix of $\mathbb{R}^{n\times n}$ and $0_{n\times m}$ is the zero matrix of $\mathbb{R}^{n\times m}$ (subscripts are omitted if obvious from context). For two matrices A, B, $\mathrm{diag}(A, B)$ is their diagonal concatenation. For two vectors a, b, $\mathrm{col}(a, b)$ is their column concatenation.

2. PROBLEM STATEMENT

Let the drive mode of a MEMS gyroscope be modeled as a second-order resonator (Sun et al., 2002):

$$G_{\omega_0}(s) = \frac{y(s)}{u(s)} = \frac{k}{(s/\omega_0)^2 + (s/\omega_0)/Q + 1}, \qquad (1)$$

where y is the displacement of the drive mode, u is the input force, k is the static gain, Q is the quality factor, and ω_0 is the resonance frequency [1] (in rad/s), which may vary slowly in the range $[\omega_{0min},\ \omega_{0max}]$ during the operation of the device. This variation is mainly caused by temperature changes, which are indeed slow. For the control design, we thus assume that ω_0 is time invariant. Furthermore, we assume that ω_0 is measured in real time. For the sake of simplicity, the quality factor is assumed to be constant as its impact is much less important than the ω_0 variations.

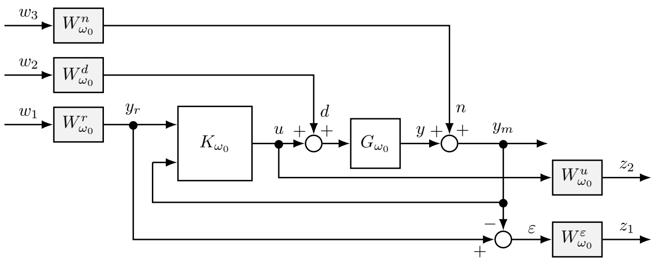

Fig. 1. H_∞ criterion.

We enumerate the control objectives:

- tracking of a sinusoidal reference signal y_r of frequency $\omega_0 \in [\omega_{0min},\ \omega_{0max}]$;
- minimization of the control effort u;
- robust stability.

Moreover, we aim to design a controller whose gains are dependent on ω_0.

In the H_∞ synthesis (for further details, see *e.g.* Skogestad and Postlethwaite (2001)), the design of the controller is formulated as an optimization problem: let an augmented plant P_{ω_0} be given by the plant G_{ω_0} and weighting functions W_{ω_0}; then, find a controller K_{ω_0}, if there is any, such that the weighted closed-loop transfer functions are stable and meet a given performance level γ, that is, $\|P_{\omega_0} \star K_{\omega_0}\|_\infty < \gamma$. Hence, the control specifications are expressed through the choice of the weighting functions and of the weighted closed-loop transfer functions.

For our application, we consider the criterion presented in Fig. 1, where we include an input disturbance d, a measurement noise n and weighting functions $W^x_{\omega_0}$, and we define $\varepsilon = y_r - y_m$ and $y_m = y + n$. Please note that the controller is composed of feedforward and feedback parts, respectively $K_{\omega_0 r}$ and $K_{\omega_0 y}$, *i.e.*, $K_{\omega_0} = [K_{\omega_0 r},\ K_{\omega_0 y}]$. The H_∞ problem is then: given a performance level $\gamma > 0$, compute a controller K_{ω_0}, if there is any, such that $\|P_{\omega_0} \star K_{\omega_0}\|_\infty < \gamma$. If this problem has a solution for $\gamma = 1$, then the following H_∞ criterion is also ensured:

$$\left\| \begin{matrix} W^\varepsilon_{\omega_0} T_{y_r\to\varepsilon} W^r_{\omega_0} & W^\varepsilon_{\omega_0} T_{d\to\varepsilon} W^d_{\omega_0} & W^\varepsilon_{\omega_0} T_{n\to\varepsilon} W^n_{\omega_0} \\ W^u_{\omega_0} T_{y_r\to u} W^r_{\omega_0} & W^u_{\omega_0} T_{d\to u} W^d_{\omega_0} & W^u_{\omega_0} T_{n\to u} W^n_{\omega_0} \end{matrix} \right\|_\infty < 1$$

with the weighting functions given by

$$W^\varepsilon_{\omega_0}(s) = \frac{1}{M_\varepsilon} \frac{(s/\omega_0)^2 + (s/\omega_0)\,\alpha_\varepsilon + 1}{(s/\omega_0)^2 + (s/\omega_0)\,\alpha_\varepsilon A_\varepsilon/M_\varepsilon + 1}, \qquad (2)$$

$$W^u_{\omega_0}(s) = M_u \frac{(s/\omega_0)^2 + (s/\omega_0)\,\alpha_u A_u/M_u + 1}{(s/\omega_0)^2 + (s/\omega_0)\,\alpha_u + 1}, \qquad (3)$$

$$W^r_{\omega_0}(s) = k_r, \quad W^d_{\omega_0}(s) = k_d \quad \text{and} \quad W^n_{\omega_0}(s) = k_n.$$

The choice of the parameters $A_\varepsilon \le 1$, $M_\varepsilon \ge 1$, α_ε, $A_u \le 1$, $M_u \ge 1$, α_u, k_r, k_d and k_n ensures the desired specifications. Details are available in Saggin et al. (2020). We can therefore formulate the control design problem.

Problem 1. Assume that ω_0 is measured in real time. Given the ω_0-dependent augmented plant P_{ω_0} and a performance level $\gamma > 0$, find a (simple-to-implement) controller K_{ω_0} that depends on ω_0, if there is any, such that, $\forall\ \omega_0 \in [\omega_{0min},\ \omega_{0max}]$, $\|P_{\omega_0} \star K_{\omega_0}\|_\infty < \gamma$.

[1] The natural frequency and the resonance one are assumed to be equal, since $Q \gg 1$ in MEMS gyroscopes.

3. PARAMETER-DEPENDENT CONTROLLER IN CONTINUOUS-TIME

In this section, we present a solution in continuous-time (CT) for Problem 1.

Note that in (1), ω_0 appears as a quotient of s. Therefore, G_{ω_0} admits a state-space representation in the form:

$$G_{\omega_0} : \begin{cases} \dot{x}(t) = \omega_0 A x(t) + \omega_0 B u(t) \\ y(t) = \quad C x(t) + \quad D u(t) \end{cases}, \tag{4}$$

where the matrices do not depend on ω_0. In this case, if we consider a representation similar to the controllable canonical form, we obtain

$$A = \begin{bmatrix} 0 & 1 \\ -1 & -1/Q \end{bmatrix}, \quad B = \begin{bmatrix} 0 \\ 1 \end{bmatrix}, \quad C = [k \ 0] \quad \text{and} \quad D = 0.$$

The same holds for the weighting functions, see (2) and (3). Thus, the augmented plant P_{ω_0} admits the state-space representation:

$$P_{\omega_0} : \begin{cases} \dot{x}_P(t) = \omega_0 A_P x_P(t) + \omega_0 B_u u(t) + \omega_0 B_w w(t) \\ y_P(t) = \quad C_y x_P(t) \qquad\qquad + \quad D_{yw} w(t) \\ z(t) = \quad C_z x_P(t) + \quad D_{zu} u(t) + \quad D_{zw} w(t) \end{cases},$$

where $x_P(t) \in \mathbb{R}^{n_P}$, $y_P(t) \in \mathbb{R}^{n_y}$, $w(t) \in \mathbb{R}^{n_w}$, $z(t) \in \mathbb{R}^{n_z}$ and whose matrices do not depend on ω_0.

At this point, we can then define a normalized Laplace variable $s_n = s/\omega_0$ and a normalized time $t_n = \omega_0 t$, such that the normalized version of P_{ω_0}, denoted P_n, is cast as

$$P_n : \begin{cases} \dot{x}_{Pn}(t_n) = A_P x_{Pn}(t_n) + \ B_u u_n(t_n) + \ B_w w_n(t_n) \\ y_{Pn}(t_n) = C_y x_{Pn}(t_n) \qquad\qquad + D_{yw} w_n(t_n) \\ z_n(t_n) = C_z x_{Pn}(t_n) + D_{zu} u_n(t_n) + D_{zw} w_n(t_n) \end{cases} \tag{5}$$

with $x_{Pn}(t_n) = x_P(t_n/\omega_0)$ and similarly for the other signals. Note that the state-space matrices of P_n do not depend on ω_0. Moreover, since $P_{\omega_0}(s) = P_n(s_n)$, $\|P_{\omega_0}\|_\infty = \|P_n\|_\infty$. Thus, the solution of Problem 1 is the solution of the standard H_∞ problem: given a normalized augmented plant P_n of (5) (see *e.g.*, Skogestad and Postlethwaite (2001)) and a performance level $\gamma > 0$, compute a normalized controller K_n, if there exists any, in the form of

$$K_n : \begin{cases} \dot{x}_{Kn}(t_n) = A_K x_{Kn}(t_n) + B_K y_{Pn}(t_n) \\ u_n(t_n) = C_K x_{Kn}(t_n) + D_K y_{Pn}(t_n) \end{cases}, \tag{6}$$

where $x_{Kn}(t_n) \in \mathbb{R}^{n_K}$, such that $\|P_n \star K_n\|_\infty < \gamma$. Hence, the CT ω_0-dependent controller K_{ω_0} is given by

$$K_{\omega_0} : \begin{cases} \dot{x}_K(t) = \omega_0 A_K x_K(t) + \omega_0 B_K y_P(t) \\ u(t) = \quad C_K x_K(t) + \quad D_K y_P(t) \end{cases}.$$

Please note that the new (denormalized) controller K_{ω_0} ensures the stability and $\|P_{\omega_0} \star K_{\omega_0}\|_\infty < \gamma$ for all $\omega_0 \in [\omega_{0min}, \ \omega_{0max}]$, *i.e.*, solves Problem 1.

4. PARAMETER-DEPENDENT CONTROLLER IN DISCRETE-TIME

We now discuss the design of a discrete-time (DT) controller whose gains depend on ω_0 and for which the discretization effects (sampling and holding) cannot be neglected.

The common procedure to design a DT controller through frequency-domain methods (as the H_∞ synthesis) is illustrated in the upper part of Fig. 2 (with no background), and described in the sequel (Åström and Wittenmark, 1997).

(1) Given a CT system G_{ω_0} with a zero-order holder (ZOH) and sampling period T_s, we compute a DT equivalent system $G^d_{\omega_0}$.
(2) A pseudo-continuous-time (PCT) system $G^p_{\varpi_0}$ is obtained through the bilinear transform. In PCT, s_p is a complex variable, which is equal to $j\varpi$ when $s = j\omega$. We denote by ϖ the pseudo-continuous frequency, given by
$$\varpi = g(\omega) \triangleq \frac{2}{T_s} \tan\left(\frac{\omega T_s}{2}\right). \tag{7}$$
(3) A PCT controller $K^p_{\varpi_0}$ is computed through a continuous-time design method.
(4) Then, the bilinear transform is applied in the other direction (from PCT to DT), and the DT controller $K^d_{\omega_0}$ is obtained.

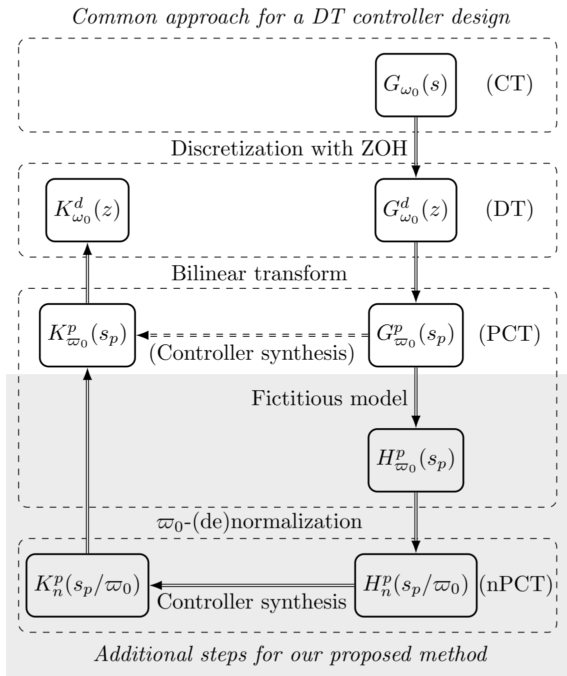

Fig. 2. Procedure for the design of a DT controller.

The main interest of this procedure is that the controller is designed in the PCT space, which has the same properties as the CT space. Thus, the choice of frequency-weighting functions and the interpretation of frequency-responses is more natural than in the DT space. However, note that the controller is based on the model $G^p_{\varpi_0}$, which is different from G_{ω_0}. Then, before applying the approach of Section 3, we need to check if $G^p_{\varpi_0}$ can be normalized such that its normalized version does not depend on ω_0.

For the system given by (1), its model in PCT, with $Q \gg 1$, can be given by (further details are available in Saggin et al. (2020)):

$$G^p_{\varpi_0}(s_p) = \frac{k\left(1 - (s_p/\varpi_0)\,\varpi_0 T_s/2\right)\left(1 + (s_p/\varpi_0)/(2Q)\right)}{(s_p/\varpi_0)^2 + (s_p/\varpi_0)/\left(Q \operatorname{sinc}(\omega_0 T_s)\right) + 1} \tag{8}$$

with $\varpi_0 = (2/T_s)\tan(\omega_0 T_s/2)$.

Note that the structure of $G^p_{\varpi_0}$ is slightly different from that of G_{ω_0}. Such differences prohibit $G^p_{\varpi_0}$ to be normalized such that it does not depend on ϖ_0 and the previous approach is not directly applicable. Hence, we propose to create a fictitious system $H^p_{\varpi_0}$ that represents a "worst-case" model of $G^p_{\varpi_0}$ for all $\omega_0 \in [\omega_{0min},\ \omega_{0max}]$ and which can be normalized. To this end, let us evaluate these modifications.

(1) The resonance frequency ϖ_0 is different from ω_0 due to the distortion caused by the bilinear transform, see (7). So, instead of normalizing $G^p_{\varpi_0}$ with respect to ω_0, it may be normalized with respect to ϖ_0.
(2) The quality factor is reduced by a factor $\mathrm{sinc}\,(\omega_0 T_s)$ due to the filtering effect of the ZOH. Then, from the performance point of view, we consider as worst case when the reduction is maximum, *i.e.*, for $\omega_0 = \omega_{0max}$.
(3) The unstable zero that appears at $s_p = 2/T_s$ has the inconvenient properties to: (i) reduce the phase of the system; and (ii) impose limitations on the closed-loop bandwidth (Freudenberg and Looze, 1985). Then, we take as worst case when this zero is closer to the resonance frequency, *i.e.*, for $\omega_0 = \omega_{0max}$.
(4) The stable zero is neglected, since it is far from ϖ_0.

Based on the above discussion, we define

$$H^p_{\varpi_0}(s_p) = \frac{k\,(1-(s_p/\varpi_0)/z_u)}{(s_p/\varpi_0)^2 + (s_p/\varpi_0)/(Q\,\mathrm{sinc}\,(\omega_{0max}T_s)) + 1} \tag{9}$$

with $z_u = (2/T_s)^2 \tan(\omega_{0max}T_s/2)$. Now, we can design a controller for $H^p_{\varpi_0}$ with the approach of Section 3. The DT controller is then obtained with the bilinear transform.

To summarize this method, we complete the scheme of Fig. 2 with the steps on a gray background, as follows.

(1) Instead of designing the controller in PCT, we define a fictitious model, $H^p_{\varpi_0}$ of (9), from the set of $G^p_{\varpi_0}$ for $\omega_0 \in [\omega_{0min},\ \omega_{0max}]$.
(2) $H^p_{\varpi_0}$ is normalized by ϖ_0, giving origin to a normalized pseudo-continuous time (nPCT) model H^p_n.
(3) Then, a normalized controller K^p_n is designed by solving a standard H_∞ problem, where P_n is defined by normalized weighting functions and H^p_n.
(4) This controller is thus denormalized by ϖ_0, generating $K^p_{\varpi_0}$.
(5) Finally, the DT controller $K^d_{\omega_0}$ is obtained by the bilinear transform of $K^p_{\varpi_0}$.

For an nPCT controller K^p_n given by the state-space matrices $(A_K,\, B_K,\, C_K,\, D_K)$, the PCT controller $K^p_{\varpi_0}$ has the state-space matrices $(\varpi_0 A_K,\, \varpi_0 B_K,\, C_K,\, D_K)$. Then, recalling that $\varpi_0 = g(\omega_0)$, the DT controller $K^d_{\omega_0}$ has the state-space matrices $(A_d(\varpi_0),\, B_d(\varpi_0),\, C_d(\varpi_0),\, D_d(\varpi_0))$ with

$$\begin{aligned} A_d\,(\varpi_0) &= (2I/T_s + \varpi_0 A_K)\,(2I/T_s - \varpi_0 A_K)^{-1} \\ B_d\,(\varpi_0) &= 4/T_s\,(2I/T_s - \varpi_0 A_K)^{-1}\,\varpi_0 B_K \\ C_d\,(\varpi_0) &= C_K\,(2I/T_s - \varpi_0 A_K)^{-1} \\ D_d\,(\varpi_0) &= D_K + C_K\,(2I/T_s - \varpi_0 A_K)^{-1}\,\varpi_0 B_K. \end{aligned} \tag{10}$$

Given that some approximations are made to obtain (8), the fictitious system $H^p_{\varpi_0}$ of (9) and, therefore, the DT controller, the following section presents a method to evaluate the performance obtained in the real system.

5. DISCRETE-TIME PARAMETER-DEPENDENT CONTROLLER VALIDATION

The previous section presents a method to design the discrete-time parameter-dependent controller. This design method relies on a fictitious model that approximates the actual plant. The first objective of this section is to evaluate if the obtained controller $K^p_{\omega_0}$ guarantees the stability and the performance specifications when it is implemented on the plant $G^p_{\varpi_0}$ for the whole operating frequency range $[\omega_{0min}, \omega_{0max}]$. For the sake of briefness, we focus on the first specification: reference tracking. We consider the problem in PCT space since stability and performance are equivalent when we apply the bilinear transformation to DT space system.

Moreover, the proposed design methods are based on the assumption that ω_0 is perfectly known. In practice, ω_0 is measured with an error that can be modeled by the measured frequency $\widehat{\omega}_0 = \omega_0 + \omega_m$, where ω_m is the mismatch between the actual frequency and the measured one. This has two consequences: (i) the controller is now parameterized by $\widehat{\omega}_0$; (ii) the reference signal oscillates at $\widehat{\omega}_0$. The analysis problem taking into account the approximations and the measurement error can therefore be stated as follows:

Problem 2. Given the closed-loop system composed of $K^p_{\widehat{\varpi}_0}$ and $G^p_{\varpi_0}$, with $\varpi_0 = g(\omega_0)$ and $\widehat{\varpi}_0 = g(\widehat{\omega}_0)$, test if $\forall\ \omega_0 \in [\omega_{0min}, \omega_{0max}]$ and $\forall\ \omega_m \in [-\omega_{m_{max}}, \omega_{m_{max}}]$, the system is stable and ensures the performance specification:

$$|T^p_{y_r \to \varepsilon}(j\widehat{\varpi}_0)| \le \eta. \tag{11}$$

Note that (11) can be dramatically simplified:

$$|T^p_{(y_r \to \varepsilon)_n}(j \cdot 1)| \le \eta. \tag{12}$$

where $T^p_{(y_r \to \varepsilon)_n}$ denotes the system $T^p_{y_r \to \varepsilon}$ with the frequency ϖ normalized by $\widehat{\varpi}_0$. In the sequel, the system is then analysed using this normalization.

Assume that ω_0 and $\widehat{\omega}_0$ are time-invariant. Since a parameter belonging to an interval can be interpreted as an uncertainty, we investigate the application of a robust analysis approach (μ-analysis framework (Skogestad and Postlethwaite, 2001)) to solve *Problem 2.* This approach is based on a particular model representation, referred to as Linear Fractional Representation (LFR) involving the Redheffer product (Zhou and Doyle, 1999), which allows isolating the uncertain part of the system from the nominal one. The first step is then to represent the system $T^p_{(y_r \to \varepsilon)_n}$, where ω_0 and ω_m are considered as uncertain parameters. Note that $T^p_{(y_r \to \varepsilon)_n}$ is the feedback interconnection of the normalized PCT system G^p_n with the controller K^p_n. Based on the CT system G_{ω_0} defined by (4), the normalized PCT system G^p_n can be described as the following feedback interconnection:

$$\begin{aligned} p(s_p/\widehat{\varpi}_0) &= \begin{bmatrix} \frac{1}{g(\omega_0+\omega_m)} I & 0 \\ 0 & e^{\omega_0 A T_s} \end{bmatrix} q(s_p/\widehat{\varpi}_0) \\ \begin{bmatrix} q(s_p/\widehat{\varpi}_0) \\ y(s_p/\widehat{\varpi}_0) \end{bmatrix} &= M^p_{Gn}(s_p/\widehat{\varpi}_0) \begin{bmatrix} p(s_p/\widehat{\varpi}_0) \\ u(s_p/\widehat{\varpi}_0) \end{bmatrix} \end{aligned},$$

that is, the following Linear Fractional Representation:

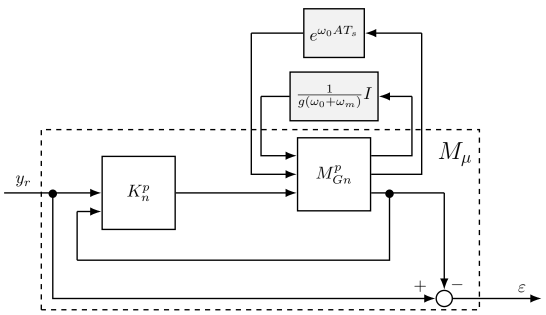

Fig. 3. Analysis scheme in nPCT space.

$$\mathrm{diag}\left(\frac{1}{g(\omega_0+\omega_m)}I, e^{\omega_0 A T_s}\right) \star M^p_{Gn}(s_p/\widehat{\varpi}_0),$$

where M^p_{Gn} is the transfer function matrix partitioned as:

$$\begin{bmatrix} q(s_p/\widehat{\varpi}_0) \\ y(s_p/\widehat{\varpi}_0) \end{bmatrix} = \begin{bmatrix} M_{Gqp}(s_p/\widehat{\varpi}_0) & M_{Gqu}(s_p/\widehat{\varpi}_0) \\ M_{Gyp}(s_p/\widehat{\varpi}_0) & M_{Gyu}(s_p/\widehat{\varpi}_0) \end{bmatrix} \begin{bmatrix} p(s_p/\widehat{\varpi}_0) \\ u(s_p/\widehat{\varpi}_0) \end{bmatrix}$$

with $q = \mathrm{col}(q_g,\ q_e)$ and $p = \mathrm{col}(p_g,\ p_e)$.

Thanks to this LFR, $T^p_{(y_r\to\varepsilon)_n}$ can be represented as in Fig. 3. From this figure, we can obtain the LFR of $T^p_{(y_r\to\varepsilon)_n}$

$$\varepsilon = \left(\left(\frac{1}{g(\omega_0+\omega_m)}I, e^{\omega_0 A T_s}\right) \star M_\mu(s_p/\widehat{\varpi}_0)\right)\right) y_r,$$

where M_μ is defined by

$$M_\mu = \begin{bmatrix} M_{Gqp} + \frac{M_{Gqu}K_{ny}M_{Gyp}}{1-M_{Gyu}K_{ny}} & \frac{M_{Gqu}K_{nr}}{1-M_{Gyu}K_{ny}} \\ -\frac{M_{Gyp}}{1-M_{Gyu}K_{ny}} & \frac{1+M_{Gyu}(K_{nr}-K_{ny})}{1-M_{Gyu}K_{ny}} \end{bmatrix} \quad (13)$$

with

$$u(s_p/\widehat{\varpi}_0) = [K_{nr}(s_p/\widehat{\varpi}_0)\ K_{ny}(s_p/\widehat{\varpi}_0)] \begin{bmatrix} y_r(s_p/\widehat{\varpi}_0) \\ y(s_p/\widehat{\varpi}_0) \end{bmatrix}.$$

Nevertheless, in order to apply the μ-analysis framework, the system has to depend on the uncertainties rationally, that is, there exist $M(s)$ such that it is represented by the LFR of the form

$$(\mathrm{diag}(\omega_0 I, \omega_m I)) \star M(s).$$

This is not our case since the dependency of $e^{\omega_0 A T_s}$ and $g(\omega_0+\omega_m)$ with respect to ω_0 and ω_m, respectively, is nonrational. To deal with this problem, we propose to approximate $e^{\omega_0 A T_s}$ and $g(\omega_0+\omega_m)$ by rational functions using Taylor series expansions. Let us introduce the following lemma.

Lemma 3. Let be a nonrational matrix function $F(\theta) \in \mathbb{R}^{n_q\times n_q}$ depending on a parameter θ, with θ taking values in a finite interval $[\theta_{min}, \theta_{max}]$ and with nominal value $\theta_c = (\theta_{max}+\theta_{min})/2$. If $F(\theta)$ is derivable $(d+1)$ times, then: $\forall\ \theta \in [\theta_{min}, \theta_{max}]$, $\exists\ \Delta_{RF} \in \mathbb{R}^{n_q\times n_q}$, $\|\Delta_{RF}\|_\infty \le R_{maxF}$ such that $F(\theta) = \mathrm{diag}(\delta_\theta I_{(d\times n_q)}, \Delta_{RF}) \star N_F$ with $\delta_\theta = \theta - \theta_c$,

$$N_F = \begin{bmatrix} 0 & \dots & 0 & 0 & I_{n_q} \\ I_{(d\times n_q)-1} & & 0 & 0 & 0 \\ 0 & \dots & 0 & 0 & I_{n_q} \\ F_1 & \dots & F_d & I_{n_q} & F_0 \end{bmatrix},$$

$F_0 = F(\theta_c)$, $F_k = F^{(k)}(\theta_c)/k!\ \forall\ k \in \{1,\dots,d\}$, and

$$R_{maxF} = \frac{D}{(d+1)!}\ (\delta_{max\theta})^{d+1}$$

with $D \ge \|F^{(d+1)}(\theta_\xi)\| \forall\ \theta_\xi \in [\theta_{min}, \theta_{max}]$, and $\delta_{max\theta} = (\theta_{max}-\theta_{min})/2$.

Proof. From the Taylor series approximation, we have that $F(\theta)$ is developed as:

$$F(\theta) = F_0 + \sum_{k=1}^{d} \delta_\theta^k F_k\ + R_F(\theta), \quad (14)$$

where $R_F(\theta)$ is the residual or error of the approximation which, since it is bounded by R_{maxF}, can be modeled as a block uncertainty. The rest of proof is obtained using the fact that $\delta_\theta^{k_i} = \prod_{k=1}^{k_i}\delta_\theta$, and rearranging the terms of (14) into an LFR form. □

Based on Lemma 3, we introduce the following Theorem allowing to test the stability and performance of $T^p_{y_r\to\varepsilon}$.

Theorem 4. Let $\underline{\Delta}$ be the set defined by:

$$\underline{\Delta} = \left\{ \Delta | \begin{array}{l} \exists\ \delta_{\omega_m} \in \mathbb{R}, \delta_{\omega_0} \in \mathbb{R}, \Delta_{Rg} \in \mathbb{R}, \Delta_{Re} \in \mathbb{R}^{n_{qe}\times n_{qe}}, \\ \Delta = \mathrm{diag}(\delta_{\omega_0} I, \delta_{\omega_m} I, \Delta_{Rg} I, \delta_{\omega_0} I, \Delta_{Re}), \\ \delta_{\omega_0} \in [\omega_{0min}, \omega_{0max}], |\delta_{\omega_m}| \le \omega_{mmax}, \\ |\Delta_{R_g}| \le R_{maxg},\ \|\Delta_{R_g}\|_\infty \le R_{maxe} \end{array} \right\}$$

If for all $\Delta \in \underline{\Delta}$, the system $\Delta \star (N \star M_\mu)$ is stable and

$$|\Delta \star (N \star M_\mu(j\times 1))| \le \eta \quad (15)$$

where M_μ is defined by (13) and $N = \mathrm{diag}(N_g, N_e)$ with

$$N_g = \begin{bmatrix} 0 & \dots & 0 & 0 & \dots & 0 & 0 & I_{n_{qg}} \\ I_{(d\times n_{qg})-1} & & 0 & I_{(d\times n_{qg})-1} & & 0 & 0 & 0 \\ 0 & \dots & 0 & 0 & \dots & 0 & 0 & I_{n_{qg}} \\ g_1 I_{n_{qg}} & \dots & g_d I_{n_{qg}} & g_1 I_{n_{qg}} & \dots & g_d I_{n_{qg}} & I_{n_{qg}} & g_0 I_{n_{qg}} \end{bmatrix}$$

$$N_e = \begin{bmatrix} 0 & \dots & 0 & 0 & I_{n_{qe}} \\ I_{(d\times n_{qe})-1} & & 0 & 0 & 0 \\ 0 & \dots & 0 & 0 & I_{n_{qe}} \\ E_1 & \dots & E_d & I_{n_{qe}} & E_0 \end{bmatrix},$$

Then $\forall\ \omega_0 \in [\omega_{0min}, \omega_{0max}]$ and $\forall\ \omega_m \in [-\omega_{m_{max}}, \omega_{m_{max}}]$, $T^p_{y_r\to\varepsilon}$ is stable and is such that (11) and (12) are satisfied.

Proof. When we apply Lemma 3 to $e^{\omega_0 A T_s}$, we obtain a rational function represented by the LFR $\mathrm{diag}(\delta_{\omega_0} I, \Delta_{Re}) \star N_e$. Similarly for $g(\widehat{\omega}_0)$ but, since $\widehat{\omega}_0 = \omega_0 + \omega_m$, then $\delta_{\widehat{\omega}_0}$ is split into δ_{ω_0} and δ_{ω_m}. Thus, applying Lemma 3 to $\mathrm{diag}(g(\widehat{\omega}_0)I, e^{\omega_0 A T_s})$ we obtain the LFR

$$\underbrace{\mathrm{diag}(\delta_{\omega_0} I, \delta_{\omega_m} I, \Delta_{Rg} I, \delta_{\omega_0} I, \Delta_{Re})}_{\Delta} \star \underbrace{\mathrm{diag}(N_g, N_e)}_{N}. \quad (16)$$

□

Remark 5. The conditions of Theorem 4 can be efficiently tested by computing the so-called μ upper bound based on the $D-G$ scalings using convex optimization involving Linear Matrix Inequalities (LMI) constraints (Scorletti et al., 2007; Ferber et al., 2015).

Remark 6. It is important to emphasize that the use of the so-called μ upper-bounds ensures stability and performance even if the uncertain parameters are slowly time-varying (Chou and Tits, 1995). The conditions of Theorem 4 then ensure stability and performance of the closed-loop system when the parameters ω_0 and ω_m are slowly time-varying, which is the case in our application.

6. NUMERICAL EXAMPLE

In this section, we illustrate the synthesis and analysis of a discrete-time parameter-dependent H_∞ controller for the drive mode of a MEMS gyroscope, as presented in

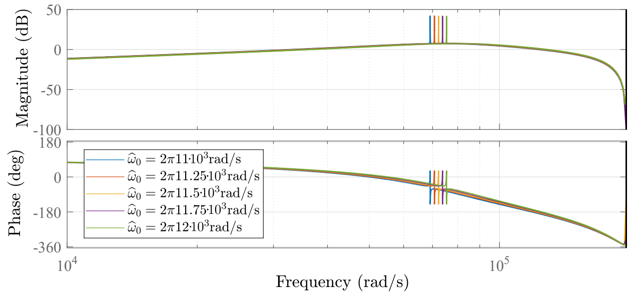

Fig. 4. Bode diagram of the feedback part of $K^d_{\widehat{\omega}_0}$ for $\widehat{\omega}_0 \in [\widehat{\omega}_{0min}, \widehat{\omega}_{0max}]$.

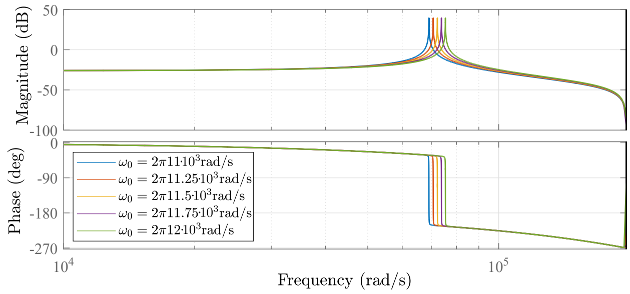

Fig. 5. Bode diagram of $G^d_{\omega_0}$ for $\omega_0 \in [\omega_{0min}, \omega_{0max}]$.

Sections 4 and 5. Its continuous-time model is given by (1) with $k = 0.05$, $Q = 2000$ and $\omega_0 \in [2\pi \cdot 11 \cdot 10^3,\ 2\pi \cdot 12 \cdot 10^3]$ rad s^{-1}. We consider the sampling period $T_s = 16 \cdot 10^{-6}$s and the following control specifications:

(1) track a reference signal $y_r(t) = Y_r \sin(\widehat{\omega}_0 t)$ with an error $\varepsilon(t) = y_r(t) - y_m(t)$ such that $|\varepsilon(t)| < 10^{-4} \cdot Y_r$ in steady-state;
(2) the control signal amplitude is less than $0.02 \cdot Y_r$ in steady-state;
(3) the closed-loop system is stable and present a modulus margin $\mathcal{M} > 1/2$.

6.1 Synthesis of a Discrete-Time Controller

Based on the control specifications above, we consider the H_∞ criterion presented in Section 2 with $M_\varepsilon = 2$, $\alpha_\varepsilon = 0.2$, $A_\varepsilon = 5 \cdot 10^{-5}$, $M_u = 400$, $\alpha_u = 1632$, $A_u = 0.004$, $k_r = 1$, $k_d = 0.05$ and $k_n = 1$ (see Saggin et al. (2020) for details on this choice).

Thus, following the method proposed in Section 4, we obtain, with $\gamma = 1.01$, a normalized controller K^p_n (see (6)). From its state-space matrices, the ω_0-dependent DT controller $K^d_{\widehat{\omega}_0}$ is computed, see (10) and (7).

We recall that the controller is composed of feedforward and feedback parts, *i.e.*, $K^d_{\widehat{\omega}_0} = [K^d_{\widehat{\omega}_0 r}, K^d_{\widehat{\omega}_0 y}]$. However, for the sake of simplicity, we focus our discussion on its feedback part, $K^d_{\widehat{\omega}_0 y}$.

The Bode diagram of $K^d_{\widehat{\omega}_0 y}$ is presented in Fig. 4. Similarly, the Bode diagram of $G^d_{\omega_0}$ is given in Fig. 5. Observe that $K^d_{\widehat{\omega}_0}$ presents a resonance peak at $\widehat{\omega}_0$, ensuring a precise reference tracking at this (varying) frequency, which coincides with the resonance peak of $G^d_{\omega_0}$ if $\widehat{\omega}_0 = \omega_0$.

We simulate $G^d_{\omega_0}$ controlled by $K^d_{\widehat{\omega}_0}$ with $Y_r = 1$ and the frequencies ω_0 and $\widehat{\omega}_0$ given in Fig. 6.

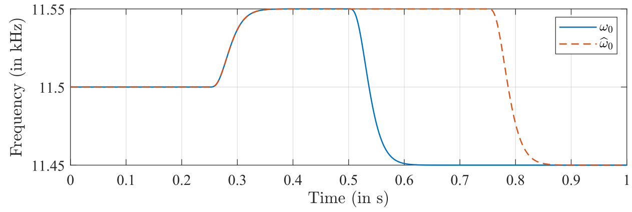

Fig. 6. Evolution of ω_0 and $\widehat{\omega}_0$ over time.

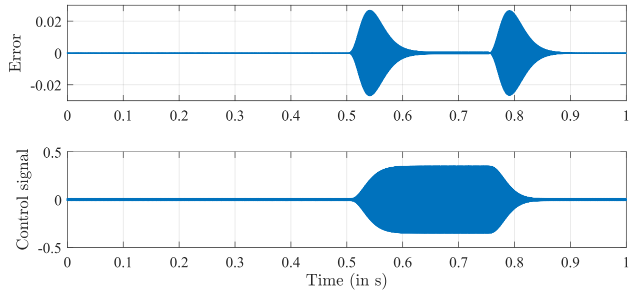

Fig. 7. Simulation results.

Table 1. Steady-state amplitude values

Time t (s)	$0 - 0.25$	$0.25 - 0.5$	$0.5 - 0.75$	$0.75 - 1$
Error	$6.5 \cdot 10^{-5}$	$6.5 \cdot 10^{-5}$	$4.6 \cdot 10^{-4}$	$6.5 \cdot 10^{-5}$
Control signal	0.01	0.01	0.35	0.01

The simulation results are presented in Fig. 7 and in Table 1. For $t < 0.5$ s, we keep $\widehat{\omega}_0(t) = \omega_0(t)$. In this interval, the specifications are verified, even when the frequencies change at $t = 0.25$ s. For the interval $0.5 < t < 0.75$ s, ω_0 changes, but $\widehat{\omega}_0$ is kept constant. In this case, the mismatch between ω_0 and $\widehat{\omega}_0$ causes a performance degradation and the initial specifications are not verified (steady-state amplitude error bigger than 10^{-4} and control signal amplitude bigger than 0.02). Finally, when $\widehat{\omega}_0$ catches back ω_0 ($t > 0.75$ s), the desired control specifications are verified again.

6.2 Performance Analysis

The first step for performance analysis is to obtain the adequate representation. To do so, we apply Lemma 3 to $e^{\omega_0 A T_s}$ and $1/g(\widehat{\omega}_0)$. We choose a Taylor truncation order $d = 2$ for both functions, in this case the maximal errors are obtained when the uncertainty is maximal, that is $R_{maxe}(\omega_{0max}) = 2.226 \cdot 10^{-5}$ and $R_{maxg}(\omega_{m_{max}}) = 2.640 \cdot 10^{-8}$. By applying Theorem 4 and putting together the repeated uncertainties, we introduce a set $\underline{\Delta} = \{\Delta \,|\Delta = \delta_{\omega_0} I_8, \Delta_{Rg} I_2, \delta_{\omega_m} I_4, \Delta_{RF}),\ \Delta_{RF} \in \mathbb{R}^{2\times 2}\}$. There is clearly a trade-off between the number of introduced uncertainties by the truncation order d of the Taylor series, and the size of the maximal approximation error, which can be translated as a trade-off between the computation time and the conservatism of the result.

We first compute the upper bound of μ to evaluate the stability of the system (16) for all $\Delta \in \underline{\Delta}$ considering a very large $\omega_{m_{max}} = 2\pi\, 500$ rad s^{-1}. We obtain a μ_{max} of 0.1923, guaranteeing then robust stability of the system (16) even in the presence of a considerable mismatch. Then, we investigate the impact of different maximal measure mismatches $\omega_{m_{max}}$ on the tracking performance specification defined in (12), for all $\omega_m \in [-\omega_{m_{max}}, \omega_{m_{max}}]$ and for

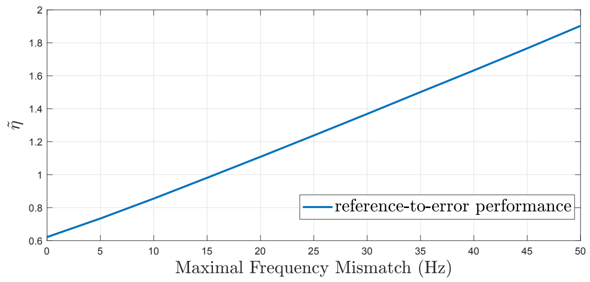

Fig. 8. Degradation of performance with respect to ω_m.

all $\omega_0 \in [\omega_{0min}, \omega_{0max}]$. We measure the performance by obtaining η through the LMI optimization problem associated to condition (15) of Theorem 4 (see Remark 5), then computing the performance ratio $\tilde{\eta} = \eta/\varepsilon_{max}$ where ε_{max} is the maximal desired tracking error. Thus, the indicator is lower than one if the performance specification is respected and greater than one if not. The obtained results are presented in Fig. 8. If we observe the particular case of $\omega_{m_{max}} = 0$, we are considering a perfect measure of the resonance frequency $\widehat{\omega}_0 = \omega_0$, which answers to the first question of Section 5. In such case, we obtain a value of $\tilde{\eta} = 0.6219$, which shows that the controller ensures performance for all $\omega_0 \in [\omega_{0min}, \omega_{0max}]$ when there is no error on the frequency measure. We also observe that $\tilde{\eta}$ increases approximately 205% for a maximal mismatch frequency of $2\pi 50\,\mathrm{rad\,s^{-1}}$, which demonstrates how performance is degraded when the measure of the resonance frequency is less accurate. Observing the maximal mismatch frequency $\omega_{m_{max}}$, for which $\tilde{\eta} = 1$, we conclude that the designed discrete-time controller ensures the tracking performance specification for all $\omega_0 \in [\omega_{0min}, \omega_{0max}]$ and for all $\omega_m \in [-\omega_{m_{max}}, \omega_{m_{max}}]$, tolerating a maximal measure error $\omega_{m_{max}}$ of $2\pi 15.763\,\mathrm{rad\,s^{-1}}$.

7. CONCLUSIONS AND PERSPECTIVES

In this work, we present an H_∞-based control design method allowing to obtain a controller whose gains depend on the MEMS gyroscope resonance frequency. The strength of our approach relies on the fact that the resonance frequency can be measured or identified. Hence, we may obtain a controller with a simple parameterization with low conservatism.

When considering a CT controller, the parameterization is straightforward. However, for the design of a DT controller, this parameterization becomes complicated (non-rational functions of ω_0 appear). Then, approximations are performed and a simple parameterization for the DT controller is revealed. The effects of these approximations are evaluated through a method based on Taylor development and μ-analysis, ensuring the performance of the system. Furthermore, examples illustrate the use and confirm the effectiveness of our proposed methods. Even if in the real application the resonance frequency varies, the computation of the μ upper-bound allows to apply our methods in the case of slow variations of ω_0.

Some perspectives may be considered: (i) implementation of the parameter-dependent controllers and integration with identification techniques; (ii) extension of the controller design for drive and sense modes in a multivariable framework; (iii) performance analysis taking into account other uncertainties, *e.g.*, the quality factor.

REFERENCES

Åström, K. and Wittenmark, B. (1997). *Computer-controlled Systems: Theory and Design*. Prentice Hall.

Chou, Y.S. and Tits, A.L. (1995). On robust stability under slowly-varying memoryless uncertainty. In *Proc IEEE Conf. Decis. Control*, volume 4, 4321–4326.

Dinh, M., Scorletti, G., Fromion, V., and Magarotto, E. (2005). Parameter dependent H_∞ control by finite dimensional LMI optimization: application to trade-off dependent control. *Int. J. Robust Nonlin.*, 15(9), 383–406.

Egretzberger, M., Mair, F., and Kugi, A. (2010). Control of vibratory mems gyroscopes based on envelope models. *IFAC Proc. Vol.*, 43(18), 441–446.

Ferber, M., Korniienko, A., Scorletti, G., Vollaire, C., Morel, F., and Krähenbühl, L. (2015). Systematic LFT derivation of uncertain electrical circuits for the worst-case tolerance analysis. *IEEE Trans. Electromagn. Compat.*, 57(5), 937–946.

Freudenberg, J. and Looze, D. (1985). Right half plane poles and zeros and design tradeoffs in feedback systems. *IEEE Trans. Autom. Control*, 30(6), 555–565.

Ljung, L. (1999). *System identification: theory for the user*. Prentice Hall, 2nd edition.

M'Closkey, R.T., Vakakis, A., and Gutierrez, R. (2001). Mode localization induced by a nonlinear control loop. *Nonlinear Dyn.*, 25(1/3), 221–236.

Oboe, R., Antonello, R., Lasalandra, E., Spinola Durante, G., and Prandi, L. (2005). Control of z-axis MEMS vibrational gyroscope. *IEEE/ASME Trans. Mechatronics*, 10(4), 364–370.

Packard, A. (1994). Gain scheduling via Linear Fractional Transformations. *Syst. Control Lett.*, 22(2), 79–92.

Saggin, F., Ayala-Cuevas, J., Korniienko, A., and Scorletti, G. (2020). On the Parameter-dependent H_∞ control for MEMS gyroscopes: synthesis and analysis. Research report, Ecole Centrale Lyon. URL `https://hal.archives-ouvertes.fr/hal-02505581`.

Saukoski, M. (2008). *System and circuit design for a capacitive MEMS gyroscope*. Ph.D. thesis, Helsinki University of Technology.

Scorletti, G., Bombois, X., Barenthin, M., and Fromion, V. (2007). Improved efficient analysis for systems with uncertain parameters. In *Proc. IEEE Conf. Decis. Control*, 5038–5043.

Scorletti, G. and El Ghaoui, L. (1998). Improved linear matrix inequality conditions for gain scheduling. In *Proc. IEEE Conf. Decis. Control*, volume 4, 3626–3631.

Skogestad, S. and Postlethwaite, I. (2001). *Multivariable feedback control - analisys and design*. John Wiley & Sons, second edition.

Sun, X., Horowitz, R., and Komvopoulos, K. (2002). Stability and Resolution Analysis of a Phase-Locked Loop Natural Frequency Tracking System for MEMS Fatigue Testing. *J. Dyn. Syst.-T ASME*, 124, 599–605.

Xia, D., Chen, S., Wang, S., and Li, H. (2009). Microgyroscope Temperature Effects and Compensation-Control Methods. *Sensors*, 9(12), 8349–8376.

Zhou, K. and Doyle, J.C. (1999). *Essentials of robust control*. Prentice Hall, Englewood Cliffs, NJ.